Quantum Electronics **49** (2) 103–110 (2019)

https://doi.org/10.1070/QEL16775

Effect of pump geometry on the generation efficiency of an alkali metal vapour laser

A.I. Parkhomenko, A.M. Shalagin

Abstract. **The influence of pump geometry on the generation efficiency of a transversely diode-pumped alkali metal vapour laser is studied theoretically. Analytical formulas describing the operation of a high-intensity laser with double-sided diode pumping in two orthogonal directions are obtained. It is shown that the generation efficiency of an alkali metal vapour laser can be increased by 8%–18% when switching from single-sided to double-sided pumping.**

Keywords: *alkali metal vapour laser, diode pumping, atomic collisions.*

1. Introduction

Diode-pumped alkali metal vapour lasers have been actively studied in recent years (see, for example, [1–6] and references therein). The great interest in these lasers is reasonably due to their potential to generate very-high-power cw radiation with a high efficiency of converting pump radiation into laser radiation. The maximum radiation power of diode-pumped alkali metal vapour lasers according to open publications has now reached (with a conversion efficiency of pump energy into laser energy of 48%) 1 kW for a caesium vapour laser [4] and 1.5 kW for a potassium vapour laser [7].

Achieving substantially higher output laser power becomes possible under transverse diode pumping. In this pump configuration, the power of the generated radiation increases in proportion to the length of the laser. The idea of a transversely diode-pumped alkali metal vapour laser was patented by Krupke et al. [8] and first implemented by Zhdanov et al. [9]. A theoretical model of the operation of such a laser was first proposed by Komashko et al. [10], where the laser operation was described by a rather complex system of differential equations solved numerically in the approximation of the effective absorption cross section of pump radiation. Compared to the model from Ref. [10], Yang et al. [11] developed a somewhat different laser model. The numerical solution of the equations in [11] was carried out under the assumption that the populations of the atomic levels of the active medium do not depend on the coordinate along the cavity axis, i.e., they are constant along the direction of propagation of the generated laser radiation. The authors of Refs [12, 13] developed an analytical model of a transversely diode-pumped alkali metal vapour, describing the operation of a laser in the practically important case of high laser intensity.

Papers [10–13] theoretically investigated the operation of an alkali metal vapour laser with single-sided transverse diode pumping. The purpose of this work is to expand the analytical model [12] to describe the generation of a high-intensity alkali metal vapour laser with double-sided transverse diode pumping. A theoretical comparison of the energy characteristics of lasers with single-sided and double-sided pumping shows that the latter makes it possible to increase the efficiency of conversion of pump radiation into laser radiation by 8%–18% and to increase the output power of laser radiation.

A.I. Parkhomenko Institute of Automation and Electrometry, Siberian Branch, Russian Academy of Sciences, prosp. Akad. Koptyuga 1, 630090 Novosibirsk, Russia; e-mail: par@iae.nsk.su;
A.M. Shalagin Institute of Automation and Electrometry, Siberian Branch, Russian Academy of Sciences, prosp. Akad. Koptyuga 1, 630090 Novosibirsk, Russia; Novosibirsk State University, ul. Pirogova 2, 630090 Novosibirsk, Russia; e-mail: shalagin@iae.nsk.su

Received 2 July 2018; revision received 6 September 2018
Kvantovaya Elektronika **49** (2) 103–110 (2019)
Translated by I.A. Ulitkin

2. Equations describing laser operation

The alkali metal vapour laser operates according to the standard three-level scheme (see, for example, [1, 2, 12]). The radiation of the pump diodes is absorbed at the D_2 transition from the ground state $^2S_{1/2}$ of the alkali metal atom to the excited state $^2P_{3/2}$. Collisions of alkali metal atoms at the $^2P_{3/2}$ level with buffer gas atoms form a population inversion at the D_1 transition ($^2P_{1/2}$–$^2S_{1/2}$), as a result of which there arises a possibility of generating laser radiation at the frequency of this transition. The levels $^2S_{1/2}$, $^2P_{1/2}$ and $^2P_{3/2}$ are denoted respectively by numbers 1, 2 and 3.

Consider the operation of an alkali metal vapour laser with single-sided and double-sided diode pumping (Fig. 1). To simplify the analysis, we assumed that the cell with alkali metal vapours and buffer gases has the form of a rectangular parallelepiped with edge lengths z_0 (length), y_0 (width) and x_0 (height). Under double-sided pumping, the laser diodes are arranged on both sides of the cell. Their radiation enters the cell in the xz plane and propagates in the y direction and in the yz plane and propagates in the x direction. For a more complete utilisation of the energy of the pump radiation, place mirrors are located on other sides of the cell, which return the pump radiation transmitted through it (the reflection coefficient of the mirrors, R_p) back to the cell. The resonator consists of two plane mirrors with reflection coefficients R_0 and R_1. Cell window transmission rates are T_0 and T_1. The energy losses in the resonator (due to diffraction of light at the edges of the mirrors, due to the geometric imperfections of the resonator, due to scattering of light in the medium by inhomogeneities) are taken into account by introducing the effective transmittance T_s. The value of T_s characterises the relative energy loss of radiation in the resonator in one pass, excluding the transmission loss of windows. It is assumed that

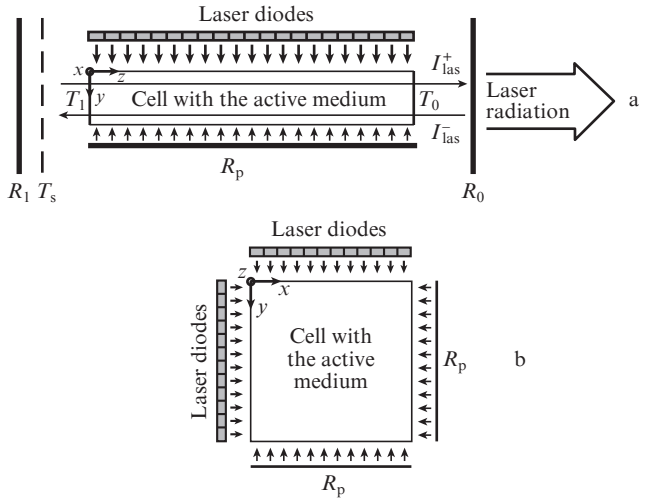

Figure 1. Scheme of an alkali metal vapour laser with (a) single-sided and (b) double-sided (laser cross-sectional view) diode pumping.

the losses of T_s are localised in front of the rear mirror R_1. The laser radiation exits the cell in the xy plane through a semitransparent mirror with a reflection coefficient R_0 and propagates in the direction of the z axis. For simplicity, we assume that the intensity distribution of pump radiation is uniform in the xz and yz planes at the input to the cell.

Under steady-state conditions with double-sided pumping, the absorption of pump radiations and the amplification of laser radiation are described by the equations:

$$\begin{aligned}
&\frac{\partial I^{\pm}_{y\omega p}(x,y,z,\omega)}{\partial y} = \mp\Big[N_1(x,y,z) - \frac{1}{2}N_3(x,y,z)\Big] \\
&\quad \times \sigma_p(\omega) I^{\pm}_{y\omega p}(x,y,z,\omega), \\
&\frac{\partial I^{\pm}_{x\omega p}(x,y,z,\omega)}{\partial x} = \mp\Big[N_1(x,y,z) - \frac{1}{2}N_3(x,y,z)\Big] \\
&\quad \times \sigma_p(\omega) I^{\pm}_{x\omega p}(x,y,z,\omega), \\
&\frac{\partial I^{\pm}_{las}(x,y,z)}{\partial z} = \mp[N_1(x,y,z) - N_2(x,y,z)] \\
&\quad \times \sigma_{las}(\omega_{las}) I^{\pm}_{las}(x,y,z).
\end{aligned} \tag{1}$$

Here, $I^{+}_{y\omega p}(x,y,z,\omega)$ and $I^{-}_{y\omega p}(x,y,z,\omega)$ are the spectral densities of the pump radiation intensity at the frequency ω, propagating along the y axis and in the opposite direction (after reflection by the mirror); $I^{+}_{x\omega p}(x,y,z,\omega)$ and $I^{-}_{x\omega p}(x,y,z,\omega)$ are the spectral densities of the pump radiation intensity at a frequency ω, propagating along the x axis and in the opposite direction (after reflection by the mirror); $I^{+}_{las}(x,y,z)$ and $I^{-}_{las}(x,y,z)$ are the intensities of laser radiation propagating along the z axis and in the opposite direction; $N_1(x,y,z)$, $N_2(x,y,z)$ and $N_3(x,y,z)$ are populations of levels 1, 2 and 3; and $\sigma_p(\omega)$ and $\sigma_{las}(\omega_{las})$ are the absorption cross sections for pump radiation and laser radiation with frequency ω_{las}, which are found by the formulas

$$\begin{aligned}
&\sigma_p(\omega) = \frac{\lambda_p^2 A_{31}}{2\pi} \frac{\Gamma_p}{\Gamma_p^2 + (\omega - \omega_{31})^2}, \\
&\sigma_{las}(\omega_{las}) = \frac{\lambda_{las}^2 A_{21}}{4\pi} \frac{\Gamma_{las}}{\Gamma_{las}^2 + (\omega_{las} - \omega_{21})^2}.
\end{aligned} \tag{2}$$

Here λ_p and λ_{las} are the centre wavelengths of the pump and laser radiations; A_{31} and A_{21} are the spontaneous emission rate (the first Einstein coefficients) for 3–1 and 2–1 transitions; $\Gamma_p = A_{31}/2 + \gamma_{31}$ and $\Gamma_{las} = A_{21}/2 + \gamma_{21}$ are the homogeneous half widths of the 3–1 and 2–1 transition lines; γ_{31} and γ_{21} are the collision half-widths of 3–1 and 2–1 transition lines; and γ_{31} and γ_{21} are the frequencies of 3–1 and 2–1 transitions. Equations (1) are supplemented by boundary conditions expressing the change in the radiation intensities on the surface of the mirrors during reflection and passage through the cell windows:

$$\begin{aligned}
&I^{+}_{y\omega p}(x,0,z,\omega) = I_{0\omega p}(\omega), \\
&I^{-}_{y\omega p}(x,y_0,z,\omega) = R_p I^{+}_{y\omega p}(x,y_0,z,\omega), \\
&I^{+}_{x\omega p}(0,y,z,\omega) = I_{0\omega p}(\omega), \\
&I^{-}_{x\omega p}(x_0,y,z,\omega) = R_p I^{+}_{x\omega p}(x_0,y,z,\omega), \\
&I^{+}_{las}(x,y,0) = R_1 T_1^2 T_s^2 I^{-}_{las}(x,y,0), \\
&I^{-}_{las}(x,y,z_0) = R_0 T_0^2 I^{+}_{las}(x,y,z_0).
\end{aligned} \tag{3}$$

Populations of levels 1, 2 and 3 in equations (1) are found from the balance equations. In the steady-state case, these equations have the form

$$\begin{aligned}
&\frac{dN_3}{dt} = 0 = -(A_{31} + \nu_{31} + \nu_{32}) N_3(x,y,z) + \nu_{23} N_2(x,y,z) \\
&\quad + w_p(x,y,z)\Big[N_1(x,y,z) - \frac{1}{2}N_3(x,y,z)\Big], \\
&\frac{dN_2}{dt} = 0 = -(A_{21} + \nu_{21} + \nu_{23}) N_2(x,y,z) + \nu_{32} N_3(x,y,z) \\
&\quad - w_{las}(x,y,z)\big[N_2(x,y,z) - N_1(x,y,z)\big], \\
&N_1(x,y,z) + N_2(x,y,z) + N_3(x,y,z) = N.
\end{aligned} \tag{4}$$

Here N is the total concentration of active atoms; collision frequencies ν_{32} and ν_{23} describe collisional mixing between levels 3 and 2; collision frequencies ν_{31} and ν_{21} describe inelastic collisional transitions through 3→1 and 2→1 channels; and $w_p(x,y,z)$ and $w_{las}(x,y,z)$ are the probabilities of induced transitions under the action of pump radiation and generated laser radiation, respectively. We assume that the pump radiation has a spectrum of arbitrary width, and the generated laser radiation is monochromatic. Then

$$\begin{aligned}
&w_p(x,y,z) = \int_0^{\infty} \frac{\sigma_p(\omega)}{\hbar\omega_p} I_{\omega p}(x,y,z,\omega)\, d\omega, \\
&w_{las}(x,y,z) = \frac{\sigma_{las}(\omega_{las})}{\hbar\omega_{las}} I_{las}(x,y,z),
\end{aligned} \tag{5}$$

where

$$\begin{aligned}
&I_{\omega p}(x,y,z,\omega) = I^{+}_{y\omega p}(x,y,z,\omega) + I^{-}_{y\omega p}(x,y,z,\omega) \\
&\quad + I^{+}_{x\omega p}(x,y,z,\omega) + I^{-}_{x\omega p}(x,y,z,\omega)
\end{aligned} \tag{6}$$

is the total spectral density of the pump radiation intensity inside the cell;

$$I_{las}(x,y,z) = I^{+}_{las}(x,y,z) + I^{-}_{las}(x,y,z) \tag{7}$$

is the total intensity of the laser radiation inside the cell; and ω_p is the centre frequency of the pump emission spectrum. The collision frequencies ν_{32} and ν_{23}, due to the principle of detailed balance, are related by the expression

$$\nu_{23} = 2\xi\nu_{32}, \quad \xi \equiv \exp[-\Delta E/(k_B T)], \tag{8}$$

where ΔE is the energy difference between levels 3 and 2; k_B is the Boltzmann constant; and T is the temperature of the gas mixture inside the cell.

From the system of algebraic equations (4) we find the population of levels:

$$\begin{aligned}
N_1(x,y,z) &= N\Big(1 + \frac{\varkappa_p \Gamma_2}{2\nu_{32} + 3\Gamma_2} + \frac{\varkappa_{las}\Gamma_3}{\nu_{23} + 2\Gamma_3} + \frac{b\varkappa_p\varkappa_{las}}{4}\Big) \\
&\quad \times (1 + \varkappa_p + \varkappa_{las} + b\varkappa_p\varkappa_{las})^{-1}, \\
N_2(x,y,z) &= N\Big(\frac{\varkappa_p \nu_{32}}{\nu_{32} + 3\Gamma_2/2} + \frac{\varkappa_{las}\Gamma_3}{\nu_{23} + 2\Gamma_3} + \frac{b\varkappa_p\varkappa_{las}}{4}\Big) \\
&\quad \times (1 + \varkappa_p + \varkappa_{las} + b\varkappa_p\varkappa_{las})^{-1}, \\
N_3(x,y,z) &= N\Big(\frac{\varkappa_p \Gamma_2}{\nu_{32} + 3\Gamma_2/2} + \frac{\varkappa_{las}\nu_{23}}{\nu_{23} + 2\Gamma_3} + \frac{b\varkappa_p\varkappa_{las}}{2}\Big) \\
&\quad \times (1 + \varkappa_p + \varkappa_{las} + b\varkappa_p\varkappa_{las})^{-1},
\end{aligned} \tag{9}$$

as well as population differences characterising laser generation and pump absorption:

$$\begin{aligned}
N_2(x,y,z) - N_1(x,y,z) &= N\frac{a\varkappa_p - 1}{1 + \varkappa_p + \varkappa_{las} + b\varkappa_p\varkappa_{las}}, \\
N_1(x,y,z) - \frac{1}{2}N_3(x,y,z) &= N\frac{1 + q\varkappa_{las}}{1 + \varkappa_p + \varkappa_{las} + b\varkappa_p\varkappa_{las}},
\end{aligned} \tag{10}$$

where

$$\begin{aligned}
&\Gamma_2 = \tilde{A}_{21} + \nu_{23}; \quad \Gamma_3 = \tilde{A}_{31} + \nu_{32}; \\
&\tilde{A}_{21} = A_{21} + \nu_{21}; \quad \tilde{A}_{31} = A_{31} + \nu_{31}; \\
&a = \frac{(1-\xi)\nu_{32} - \tilde{A}_{21}/2}{(1+3\xi)\nu_{32} + 3\tilde{A}_{21}/2}; \quad q = \frac{(1-\xi)\nu_{32} + \tilde{A}_{31}}{2[(1+\xi)\nu_{32} + \tilde{A}_{31}]}; \\
&b = \frac{(\tilde{A}_{21} + 2\xi\tilde{A}_{31})\nu_{32} + \tilde{A}_{21}\tilde{A}_{31}}{[(1+\xi)\nu_{32} + \tilde{A}_{31}][(1+3\xi)\nu_{32} + 3\tilde{A}_{21}/2]};
\end{aligned} \tag{11}$$

$\tilde{A}_{31}$ and $\tilde{A}_{21}$ are the transition frequencies from levels 3 and 2 as a result of spontaneous emission and collisional transitions to the ground state; and Γ_3 and Γ_2 are the total transition frequencies from levels 3 and 2 as a result of spontaneous emission and collisions. The quantities $\varkappa_p \equiv \varkappa_p(x,y,z)$ and $\varkappa_{las} \equiv \varkappa_{las}(x,y,z)$ are defined as

$$\begin{aligned}
&\varkappa_p = \frac{w_p(x,y,z)}{\beta_p}, \quad \varkappa_{las} = \frac{w_{las}(x,y,z)}{\beta_{las}}, \\
&\beta_p = \frac{(\tilde{A}_{21} + 2\xi\tilde{A}_{31})\nu_{32} - \tilde{A}_{21}\tilde{A}_{31}}{(1+3\xi)\nu_{32} + 3\tilde{A}_{21}/2}, \\
&\beta_{las} = \frac{(\tilde{A}_{21} + 2\xi\tilde{A}_{31})\nu_{32} + \tilde{A}_{21}\tilde{A}_{31}}{2[(1+\xi)\nu_{32} + \tilde{A}_{31}]}
\end{aligned} \tag{12}$$

and denote the saturation parameters, since each of them characterises the degree of population equalisation at the 3–1 or 2–1 transition in the absence of the second field.

Taking into account relations (10), the differential equations (1), describing the operation of a laser, take the form:

$$\begin{aligned}
\frac{\partial I^{\pm}_{y\omega p}(x,y,z,\omega)}{\partial y} &= \mp\frac{(1 + q\varkappa_{las})N\sigma_p(\omega)I^{\pm}_{y\omega p}(x,y,z,\omega)}{1 + \varkappa_p + \varkappa_{las} + b\varkappa_p\varkappa_{las}}, \\
\frac{\partial I^{\pm}_{x\omega p}(x,y,z,\omega)}{\partial x} &= \mp\frac{(1 + q\varkappa_{las})N\sigma_p(\omega)I^{\pm}_{x\omega p}(x,y,z,\omega)}{1 + \varkappa_p + \varkappa_{las} + b\varkappa_p\varkappa_{las}}, \\
\frac{\partial I^{\pm}_{las}(x,y,z)}{\partial z} &= \pm\frac{(a\varkappa_p - 1)N\sigma_{las}(\omega_{las})I^{\pm}_{las}(x,y,z)}{1 + \varkappa_p + \varkappa_{las} + b\varkappa_p\varkappa_{las}}.
\end{aligned} \tag{13}$$

As follows from the equations for $I^{\pm}_{las}$ in (13), lasing occurs when the condition $a\varkappa_p > 1$ is satisfied. To ensure effective generation ($a\varkappa_p \gg 1$), one must meet the conditions

$$\nu_{32} \gg \tilde{A}_{21}, \tilde{A}_{31}, \quad \varkappa_p \gg \frac{1+3\xi}{1-\xi}. \tag{14}$$

The first condition in (14) is satisfied with a large margin at a sufficiently high pressure of the buffer gas (~1 atm and higher). To fulfil the second condition, the spectral power density of pump radiation must be sufficiently high. Under these conditions, pumping produces an extremely large population inversion at the laser transition.

3. Relationship between the integral characteristics of radiations

The system of differential equations (13) describing the laser operation can be solved only by numerical methods. Nevertheless, it is possible, without solving it, to obtain a practically important relationship between the integral characteristics of radiations.

For the power of laser radiation generated inside the cell, from the second equation in (4), taking into account the first formula in (10) we obtain the expression (integration is performed over the cell volume):

$$\begin{aligned}
P^{cell}_{las} &= \hbar\omega_{las}\int\omega_{las}(N_2 - N_1)\,dV \\
&= N\hbar\omega_{las}\beta_{las}\int_0^{x_0}dx\int_0^{y_0}dy\int_0^{z_0}dz\frac{\varkappa_{las}(a\varkappa_p - 1)}{1 + \varkappa_p + \varkappa_{las} + b\varkappa_p\varkappa_{las}}.
\end{aligned} \tag{15}$$

Hereafter, we assume that in the considered geometry of the transversely pumped laser, the laser radiation is generated in the entire volume of the cell, $V = x_0 y_0 z_0$. For further calculations, we need another expression for the power of laser radiation generated inside the cell:

$$\begin{aligned}
P^{cell}_{las} &= \int_0^{x_0}dx\int_0^{y_0}dy[I^{+}_{las}(x,y,z_0) - I^{-}_{las}(x,y,z_0) \\
&\quad + I^{-}_{las}(x,y,0) - I^{+}_{las}(x,y,0)].
\end{aligned} \tag{16}$$

The intensity $I^{out}_{las}(x,y)$ of the laser radiation emerging from the resonator through a semi-transparent mirror with a reflection coefficient R_0 is given by the expression

$$I^{out}_{las}(x,y) = T_0(1 - R_0)I^{+}_{las}(x,y,z_0). \tag{17}$$

The power P_{las}^{out} of the laser radiation emerging from the resonator through a semitransparent mirror is defined as the integral of the intensity over the beam cross section:

$$P_{las}^{out} = \int_0^{x_0} dx \int_0^{y_0} I_{las}^{out}(x,y)\,dy. \quad (18)$$

Let us find the relation between the powers P_{las}^{out} (18) and P_{las}^{cell} (15). From the last two equations in (13) we obtain

$$\frac{1}{I_{las}^{+}(x,y,z)}\frac{\partial I_{las}^{+}(x,y,z)}{\partial z} = -\frac{1}{I_{las}^{-}(x,y,z)}\frac{\partial I_{las}^{-}(x,y,z)}{\partial z}, \quad (19)$$

from which it follows that the product $I_{las}^{+}(x,y,z)I_{las}^{-}(x,y,z)$ does not depend on z. In particular, the relation

$$I_{las}^{+}(x,y,z_0)I_{las}^{-}(x,y,z_0) = I_{las}^{+}(x,y,0)I_{las}^{-}(x,y,0). \quad (20)$$

For the integrand in (16) with (17), (20) and boundary conditions (3) taken into account, we obtain

$$I_{las}^{+}(x,y,z_0) - I_{las}^{-}(x,y,z_0) + I_{las}^{-}(x,y,0) - I_{las}^{+}(x,y,0) = I_{las}^{out}(x,y)/R, \quad (21)$$

where

$$R = \frac{T_0(1-R_0)\sqrt{\tilde{R}_l}}{(1-\tilde{R}_0)\sqrt{\tilde{R}_l} + (1-\tilde{R}_l)\sqrt{\tilde{R}_0}}, \qquad \tilde{R}_0 = R_0 T_0^2, \quad \tilde{R}_l = R_l T_l^2 T_s^2. \quad (22)$$

Expressions (15), (16), (18) and (21) yield the relationship between the powers P_{las}^{out} and P_{las}^{cell} (15):

$$P_{las}^{out} = RP_{las}^{cell} = RN\hbar\omega_{las}\beta_{las}\int_0^{x_0}dx\int_0^{y_0}dy\int_0^{z_0}dz\frac{\varkappa_{las}(a\varkappa_p - 1)}{1+\varkappa_p+\varkappa_{las}+b\varkappa_p\varkappa_{las}}. \quad (23)$$

For the absorbed pump radiation power, from the first equation in (4) taking into account the second formula in (10) we obtain the expression:

$$P_{abs} = \hbar\omega_p\int w_p\left(N_l - \frac{1}{2}N_3\right)dV = N\hbar\omega_p\beta_p\int_0^{x_0}dx\int_0^{y_0}dy\int_0^{z_0}dz\frac{\varkappa_p(1+q\varkappa_{las})}{1+\varkappa_p+\varkappa_{las}+b\varkappa_p\varkappa_{las}}. \quad (24)$$

Then, we take into account that the total pump power loss for spontaneous emission and quenching by collisions in the cell volume is given by the fairly obvious expression:

$$P_{loss} = \hbar\omega_p\int(N_2\tilde{A}_{21} + N_3\tilde{A}_{31})\,dV = N\hbar\omega_p\int_0^{x_0}dx\int_0^{y_0}dy\int_0^{z_0}dz \times\frac{\beta_p\varkappa_p + \beta_{las}\varkappa_{las} + \varkappa_p\varkappa_{las}b(\tilde{A}_{21}+2\tilde{A}_{31})/4}{1+\varkappa_p+\varkappa_{las}+b\varkappa_p\varkappa_{las}}. \quad (25)$$

From (23), (24) and (25) we obtain the expression

$$P_{las}^{out} = R\frac{\omega_{las}}{\omega_p}(P_{abs} - P_{loss}), \quad (26)$$

relating the laser output power P_{las}^{out} coupled out from the resonator with the absorbed pump power P_{abs} and the pump power loss P_{loss} due to spontaneous emission and quenching collisions.

4. High intensity of laser radiation

The system of differential equations (13) describing the laser operation can be solved in general only numerically. However, for the case of a high laser radiation intensity and a sufficiently high buffer gas pressure, which is reduced to the fulfilment of conditions

$$\varkappa_{las} \gg 1 + \varkappa_p + b\varkappa_p\varkappa_{las}, \quad \varkappa_{las} \gg 1/q, \quad (27)$$

equation (13) is simplified and allows an analytical solution. The first condition means both a high intensity of laser radiation (a large saturation parameter $\varkappa_{las}$, not only in comparison with unity, but also in comparison with a saturation parameter for pump radiation $\varkappa_p$) and a high pressure ensuring a small parameter b such that $b\varkappa_p \ll 1$. In order to satisfy the second condition in (27), a sufficiently large saturation parameter $\varkappa_{las}$ (in particular, for rubidium atoms $1/q \approx 5$) is also needed.

On the basis of approximation (27), we leave in equations (13) only $\varkappa_{las}$ in denominators and discard unity in the first and second equations (13) in numerators in comparison with $q\varkappa_{las}$. As a result, when conditions (27) are fulfilled, differential equations (13) take the form:

$$\frac{\partial I_{y\omega p}^{\pm}(y,\omega)}{\partial y} = \mp qN\sigma_p(\omega)I_{y\omega p}^{\pm}(y,\omega),$$
$$\frac{\partial I_{x\omega p}^{\pm}(x,\omega)}{\partial x} = \mp qN\sigma_p(\omega)I_{x\omega p}^{\pm}(x,\omega),$$
$$\frac{\partial I_{las}^{\pm}(x,y,z)}{\partial z} = \pm N\beta_{las}\hbar\omega_{las}[a\varkappa_p(x,y) - 1] \times\frac{I_{las}^{\pm}(x,y,z)}{I_{las}^{+}(x,y,z) + I_{las}^{-}(x,y,z)}, \quad (28)$$

where the saturation parameter $\varkappa_p$ is independent of the coordinate z and is given, in accordance with (5), (6) and (12), by the expression

$$\varkappa_p(x,y) = \frac{1}{\beta_p\hbar\omega_p}\int_0^{\infty}\sigma_p(\omega)[I_{y\omega p}^{+}(y,\omega) + I_{y\omega p}^{-}(y,\omega) + I_{x\omega p}^{+}(x,\omega) + I_{x\omega p}^{-}(x,\omega)]\,d\omega. \quad (29)$$

Solving the equations for the laser radiation intensities in (28) with allowance for the boundary conditions (3), we obtain

$$I_{las}^{\pm}(x,y,z) = \frac{I_{las}(x,y,z)}{2} \pm \frac{N}{2}\beta_{las}\hbar\omega_{las}[a\varkappa_p(x,y) - 1] \times\left[z - z_0\frac{(1-\tilde{R}_l)\sqrt{\tilde{R}_0}}{(1-\tilde{R}_0)\sqrt{\tilde{R}_l} + (1-\tilde{R}_l)\sqrt{\tilde{R}_0}}\right], \quad (30)$$

where $I_{las}(x,y,z)$ is the total intensity of laser radiation inside the cell, determined by the formula

$$I_{las}(x,y,z) \equiv I^{+}_{las}(x,y,z) + I^{-}_{las}(x,y,z)$$
$$= N\beta_{las}\hbar\omega_{las}[a\varkappa_p(x,y) - 1]$$
$$\times\left\{\left[z - z_0\frac{(1-\tilde{R}_l)\sqrt{\tilde{R}_0}}{(1-\tilde{R}_0)\sqrt{\tilde{R}_l} + (1-\tilde{R}_l)\sqrt{\tilde{R}_0}}\right]^2\right.$$
$$\left. + z_0^2\frac{4\tilde{R}_0\tilde{R}_l}{\left[(1-\tilde{R}_0)\sqrt{\tilde{R}_l} + (1-\tilde{R}_l)\sqrt{\tilde{R}_0}\right]^2}\right\}^{1/2}. \quad (31)$$

If the effective reflection coefficients of the mirrors, $\tilde{R}_0$ and $\tilde{R}_l$, are close to unity, then, according to (31), the laser radiation intensity I_{las} inside the cell is almost constant along the z axis of the resonator. From formulas (17) and (30) we find the laser output intensity:

$$I^{out}_{las}(x,y) = RNz_0\beta_{las}\hbar\omega_{las}[a\varkappa_p(x,y) - 1], \quad (32)$$

where R is given by formula (22).

Next, to solve the problem, we need to find the saturation parameter $\varkappa_p(x,y)$, determined by the first two equations for the spectral densities of the pump radiation intensity, $I^{\pm}_{y\omega p}(y,\omega)$ и $I^{\pm}_{x\omega p}(x,\omega)$, in (28). The solution of the first two equations (28) taking into account the boundary conditions (3) is not difficult:

$$\begin{aligned}
&I^{+}_{y\omega p}(y,\omega) = I_{0\omega p}(\omega)\exp[-qN\sigma_p(\omega)y],\\
&I^{-}_{y\omega p}(y,\omega) = R_p I_{0\omega p}(\omega)\exp[-qN\sigma_p(\omega)(2y_0 - y)],\\
&I^{+}_{x\omega p}(x,\omega) = I_{0\omega p}(\omega)\exp[-qN\sigma_p(\omega)x],\\
&I^{-}_{x\omega p}(x,\omega) = R_p I_{0\omega p}(\omega)\exp[-qN\sigma_p(\omega)(2x_0 - x)].
\end{aligned} \quad (33)$$

According to (33), the spectral density of the pump radiation intensity passing through the cell medium decreases exponentially. This circumstance is due to the fact that under conditions (27) the population difference of the levels $N_1 - {}^1\!/_2 N_3$, which characterises the absorption of the pump, does not depend on the intensities of the pump radiation and laser radiation: $N_1 - {}^1\!/_2 N_3 = qN$.

For the absorbed pump radiation power in the cell volume, from expression (24), when conditions (27) are satisfied, we obtain

$$P_{abs} = q\hbar\omega_p\beta_p Nz_0\int_0^{x_0}dx\int_0^{y_0}dy\,\varkappa_p(x,y). \quad (34)$$

For the pump power loss due to spontaneous emission and collisional quenching in the cell volume, from expression (25), when conditions (27) are fulfilled, we find

$$P_{loss} = NV\hbar\omega_p\beta_{las}, \quad (35)$$

where $V = x_0y_0z_0$ is the volume of the cell with the active medium.

The resulting analytical formulas (29)–(35) describe the operation of a high-intensity transversely diode-pumped alkali metal vapour laser and allow any energy characteristics of the laser to be exhaustively determined.

5. Analysis of lasing characteristics

To further elaborate the calculations using the above formulas, it is necessary to specify the spectral density of the radiation intensity $I_{0\omega p}(\omega)$ of the pump diodes at the input to the cell. We assume that at the cell input the pump emission spectrum is Gaussian:

$$I_{0\omega p}(\omega) = \frac{I_{0p}}{\sqrt{\pi}\Delta\omega}\exp\left[-\left(\frac{\omega-\omega_p}{\Delta\omega}\right)^2\right],\ \ I_{0p} = \int_0^\infty I_{0\omega p}(\omega)\,d\omega, \quad (36)$$

where I_{0p} is the pump radiation intensity at the input to the cell, and $\Delta\omega$ is the half width (at the 1/e level) of the pump emission spectrum.

From (33), taking into account (36), for the total spectral density of the pump radiation intensity $I_{\omega p}(x,y,\omega)$ inside the cell, we obtain

$$\begin{aligned}
&I_{\omega p}(x,y,\omega) = I_{y\omega p}(y,\omega) + I_{x\omega p}(x,\omega),\\
&I_{y\omega p}(y,\omega) = I^{+}_{y\omega p}(y,\omega) + I^{-}_{y\omega p}(y,\omega)\\
&\quad = \frac{I_{0p}}{\sqrt{\pi}\Delta\omega}\{\exp[-g(\omega,y)] + R_p\exp[-g(\omega,2y_0 - y)]\},\\
&I_{x\omega p}(x,\omega) = I^{+}_{x\omega p}(x,\omega) + I^{-}_{x\omega p}(x,\omega)\\
&\quad = \frac{I_{0p}}{\sqrt{\pi}\Delta\omega}\{\exp[-g(\omega,x)] + R_p\exp[-g(\omega,2x_0 - x)]\},\\
&g(\omega,y) = \left(\frac{\omega-\omega_p}{\Delta\omega}\right)^2 + q\sigma_p(\omega)Ny,\\
&g(\omega,x) = \left(\frac{\omega-\omega_p}{\Delta\omega}\right)^2 + q\sigma_p(\omega)Nx.
\end{aligned} \quad (37)$$

Then, the total intensity of the pump radiation inside the cell is:

$$\begin{aligned}
&I_p(x,y) = I_{yp}(y) + I_{xp}(x),\\
&I_{yp}(y) = \int_0^\infty I_{y\omega p}(y,\omega)\,d\omega = I_{0p}[f_1(y) + R_p f_1(2y_0 - y)],\\
&I_{xp}(x) = \int_0^\infty I_{x\omega p}(x,\omega)\,d\omega = I_{0p}[f_1(x) + R_p f_1(2x_0 - x)],\\
&f_1(y) = \frac{1}{\sqrt{\pi}\Delta\omega}\int_0^\infty \exp[-g(\omega,y)]\,d\omega,\\
&f_1(x) = \frac{1}{\sqrt{\pi}\Delta\omega}\int_0^\infty \exp[-g(\omega,x)]\,d\omega.
\end{aligned} \quad (38)$$

The saturation parameters $\varkappa_{las}(x,y,z)$ and $\varkappa_p(x,y)$ in the conditions under consideration are given by the expressions:

$$\begin{aligned}
&\varkappa_{las}(x,y,z) = \frac{\sigma_{las}(\omega_{las})}{\beta_{las}\hbar\omega_{las}}I_{las}(x,y,z),\\
&\varkappa_p(x,y) = \varkappa_{yp}(y) + \varkappa_{xp}(x),\\
&\varkappa_{yp}(y) = \frac{\sigma_p(\omega_{31})}{\beta_p\hbar\omega_p}I_{0p}[f_2(y) + R_p f_2(2y_0 - y)],\\
&\varkappa_{xp}(x) = \frac{\sigma_p(\omega_{31})}{\beta_p\hbar\omega_p}I_{0p}[f_2(x) + R_p f_2(2x_0 - x)],\\
&f_2(y) = \frac{1}{\sqrt{\pi}\Delta\omega}\int_0^\infty \frac{\exp[-g(\omega,y)]}{1 + [(\omega-\omega_{31})/\Gamma_p]^2}\,d\omega,\\
&f_2(x) = \frac{1}{\sqrt{\pi}\Delta\omega}\int_0^\infty \frac{\exp[-g(\omega,x)]}{1 + [(\omega-\omega_{31})/\Gamma_p]^2}\,d\omega.
\end{aligned} \quad (39)$$

For the absorbed pump radiation power, from expression (34) with allowance for formulas (38) and (39), we obtain the relation

$$P_{\text{abs}} = P_{y0\text{p}}\{1 - f_1(y_0) + R_\text{p}[f_1(y_0) - f_1(2y_0)]\} + P_{x0\text{p}}\{1 - f_1(x_0) + R_\text{p}[f_1(x_0) - f_1(2x_0)]\}, \quad (40)$$

where $P_{y0\text{p}} = x_0 z_0 I_{0\text{p}}$ and $P_{x0\text{p}} = y_0 z_0 I_{0\text{p}}$ are the pump radiation powers at the cell input, respectively, propagating in the direction of the y axis (in the xz plane) and in the direction of the x axis (in the yz plane). From formula (26) using (40), (35) we obtain the expression for the laser power couple out from the resonator:

$$P_{\text{las}}^{\text{out}} = R\frac{\omega_{\text{las}}}{\omega_\text{p}}(P_{y0\text{p}}\{1 - f_1(y_0) + R_\text{p}[f_1(y_0)] - f_1(2y_0)]\} + P_{x0\text{p}}\{1 - f_1(x_0) + R_\text{p}[f_1(x_0) - f_1(2x_0)]\}) - RNV\hbar\omega_{\text{las}}\beta_{\text{las}}. \quad (41)$$

For the ratio of the laser power from the resonator to the pump radiation power, which characterises the efficiency of conversion of the pump radiation into laser radiation, we obtain

$$\frac{P_{\text{las}}^{\text{out}}}{P_{0\text{p}}} = R\frac{\omega_{\text{las}}}{\omega_\text{p}}\left(\frac{x_0}{x_0 + y_0}\{1 - f_1(y_0) + R_\text{p}[f_1(y_0) - f_1(2y_0)]\} + \frac{y_0}{x_0 + y_0}\{1 - f_1(x_0) + R_\text{p}[f_1(x_0) - f_1(2x_0)]\}\right) - \frac{RNV\hbar\omega_{\text{las}}\beta_{\text{las}}}{(x_0 + y_0)z_0 I_{0\text{p}}}, \quad (42)$$

where $P_{0\text{p}} = P_{y0\text{p}} + P_{x0\text{p}} = (x_0 + y_0)z_0 I_{0\text{p}}$ is the total power of pump radiation at the input to the cell under double-sided pumping.

The above formulas (40)–(42) refer to the case of a double-sided diode pumped laser. To compare the energy characteristics of single-side and double-side-pumped lasers, we present the corresponding formulas for the case of a single-side-pumped laser (in formulas (40)–(42), we assume $P_{x0\text{p}} = 0$, $P_{0\text{p}} = P_{y0\text{p}}$):

$$P_{\text{abs}} = P_{y0\text{p}}\{1 - f_1(y_0) + R_\text{p}[f_1(y_0) - f_1(2y_0)]\},$$

$$P_{\text{las}}^{\text{out}} = R\frac{\omega_{\text{las}}}{\omega_\text{p}}P_{y0\text{p}}\{1 - f_1(y_0) + R_\text{p}[f_1(y_0) - f_1(2y_0)]\} - RNV\hbar\omega_{\text{las}}\beta_{\text{las}}, \quad (43)$$

$$\frac{P_{\text{las}}^{\text{out}}}{P_{0\text{p}}} = R\frac{\omega_{\text{las}}}{\omega_\text{p}}\{1 - f_1(y_0) + R_\text{p}[f_1(y_0) - f_1(2y_0)]\} - \frac{RNV\hbar\omega_{\text{las}}\beta_{\text{las}}}{x_0 z_0 I_{0\text{p}}}.$$

It can be clearly seen from formulas (42), (43) that the efficiency of generation of an alkali metal vapour laser under double-sided pumping is higher than that under single-sided pumping. The increase in generation efficiency is maximal if the height and width of the cell with alkali metal vapours are equal (at $x_0 = y_0$).

Let us clarify the physical reasons for an increase in the efficiency of laser generation during the transition from single-sided pumping to double-sided pumping. Under conditions (27) of a high intensity of laser radiation and a high enough pressure of a buffer gas (such as to ensure that the condition of high rate of collisional mixing between levels 3 and 2, $\nu_{32} \gg \tilde{A}_{21}, \tilde{A}_{31}$), the populations of excited levels 2 and 3 do not depend on the intensity of pump radiation and laser radiation: $N_2 = N\Gamma_3/(\nu_{23} + 2\Gamma_3)$, $N_3 = N\nu_{23}/(\nu_{23} + 2\Gamma_3)$, and therefore the total pump power loss P_{loss} due to spontaneous emission and collisional quenching in the cell volume (35) does not depend on the pump radiation power. As a result, with an increase in the pump radiation power, a large proportion of it is converted into laser radiation. Finally, the conversion efficiency of pump radiation into laser radiation increases with increasing radiation power of the pump diodes, i.e., the efficiency increases with the transition from single-sided pumping to double-sided one.

We note here the following important circumstance. The right-hand side of the formula for $P_{\text{las}}^{\text{out}}/P_{0\text{p}}$ in (43) contains the concentration N of active particles and the cell width y_0 only in combination Ny_0. This means that when $Ny_0 = \text{const}$, a change in the cell width does not affect the generation efficiency of a single-sided diode-pumped alkali metal vapour laser. For a double-sided diode pumped laser in the case of a square cell cross section (at $x_0 = y_0$), the generation efficiency, as can be seen from formula (42), also depends on the parameter Ny_0.

Let us calculate the energy characteristics of a single-sided and double-sided diode pumped laser using the above formulas. The active medium in the laser cell consists of rubidium atoms, and a mixture of helium and methane is used as a buffer gas. Methane is usually used for efficient collisional mixing between excited levels 3 and 2 in alkali metal atoms [1]. Helium is added to increase the collisional broadening of the D_2 line in order to more efficiently use the broadband radiation of the pump diodes [1].

Let us specify the initial data necessary for the calculation of the laser operation. For rubidium atoms, according to the NIST database [14], the rates of radiative transitions are $A_{21} = 3.6\times10^7$ s^{-1}, $A_{31} = 3.8\times10^7$ s^{-1}, the transition wavelengths are $\lambda_{21} = 794.8$ nm, $\lambda_{31} = 780.0$ nm and the energy difference ΔE between levels 3 and 2 is 237.6 cm^{-1}. The collisional broadenings for rubidium atoms in a buffer gas are as follows [15]: in helium, $\gamma_{\text{He}(D_1)} = 9.45$ MHz Torr^{-1} for the D_1 line and $\gamma_{\text{He}(D_2)} = 10.0$ MHz Torr^{-1} for the D_2 line; and in methane, $\gamma_{\text{CH}_4(D_1)} = 14.55$ MHz Torr^{-1} for the D_1 line and $\gamma_{\text{CH}_4(D_2)} = 13.1$ MHz Torr^{-1} for the D_2 line.

To find the collision frequency ν_{32}, we use the following cross sections for the collisional transitions between the fine components of the excited state of rubidium atoms: $\sigma_{32(\text{He})} = 0.103\times10^{-16}$ cm^2 in helium [16] and $\sigma_{32(\text{CH}_4)} = 42\times10^{-16}$ cm^2 in methane [17]. Because of the small cross section $\sigma_{32(\text{He})}$, a molecular gas is added to the buffer mixture.

For cross sections $\sigma_{31(\text{CH}_4)}$ and $\sigma_{21(\text{CH}_4)}$ of the collisional quenching of excited levels 3 and 2 of rubidium atoms interacting with methane, Zameroski et al. [18] experimentally obtained the values not exceeding 1.9×10^{-18} cm^2. In calculating the collision frequencies ν_{31} and ν_{21}, we assumed that $\sigma_{31(\text{CH}_4)} = \sigma_{21(\text{CH}_4)} = 1.9\times10^{-18}$ cm^2. For rubidium atoms colliding with helium atoms, the collisional quenching cross sections are extremely small ($\sigma_{31(\text{He})}$, $\sigma_{21(\text{He})} \leqslant 3\times10^{-20}$ cm^2 [19]), and therefore quenching due to interaction with helium can be neglected.

We assume below in the calculation that the centre frequency of the pump emission spectrum and the laser radiation frequency coincide with the frequencies of 3–1 and 2–1 transitions, respectively: $\omega_p = \omega_{31}$, $\omega_{las} = \omega_{21}$. The cell should be designed in such a way that the alkali metal vapour enters it through the side branches so that the concentration N of active particles inside the cell is set by the temperature of these branches containing an alkali metal and is not related to the temperature T of the gas mixture inside the cell. For a double-sided diode-pumped laser, we assume that the cell with alkali metal vapors has a square cross section, i.e., $x_0 = y_0$.

According to previous studies [12, 13], the efficiency of conversion of pump radiation into laser radiation, P_{las}^{out}/P_{0p}, depends nonmonotonically on the parameter Ny_0 and on the pressures of helium p_{He} and methane p_{CH_4}; the conversion efficiency reaches its maximum value $(P_{las}^{out}/P_{0p})_{max}$ at some optimal parameter $(Ny_0)_{opt}$ and some optimal pressures p_{He}^{opt} and $p_{CH_4}^{opt}$ of helium and methane. When the values of Ny_0, p_{He} and p_{CH_4} deviate from their optimal values in the direction of their increase or decrease, the efficiency of the laser operation decreases noticeably. We draw attention to the following important circumstance. The numerical analysis shows that at a given average spectral intensity $I_{0p}/\Delta\omega$ of pump radiation and at optimal values of $(Ny_0)_{opt}$, p_{He}^{opt} and $p_{CH_4}^{opt}$, the generation efficiency is the same at different $\Delta\omega$.

Figure 2 shows the results of calculations of $(P_{las}^{out}/P_{0p})_{max}$ using formulas (42) and (43) for single-sided and double-sided diode pumped lasers as functions of the average spectral intensity $I_{0p}/[\Delta\omega/(2\pi c)]$ of the pump radiation at optimal parameters $(Ny_0)_{opt}$ and optimal helium pressures p_{He}^{opt}. The optimum pressure of the methane buffer gas is 0.5–1 atm; in the calculations, the methane pressure p_{CH_4} was assumed to be 1 atm. The results of calculations of the dependence of the optimal helium pressure p_{He}^{opt} and the optimal parameter $(Ny_0)_{opt}$ on the half-width of the pump emission spectrum $\Delta\omega/(2\pi c)$ at three values of the average spectral intensity of the pump radiation of 0.5, 1 and 2 kW cm^{-1} is shown in Fig. 3.

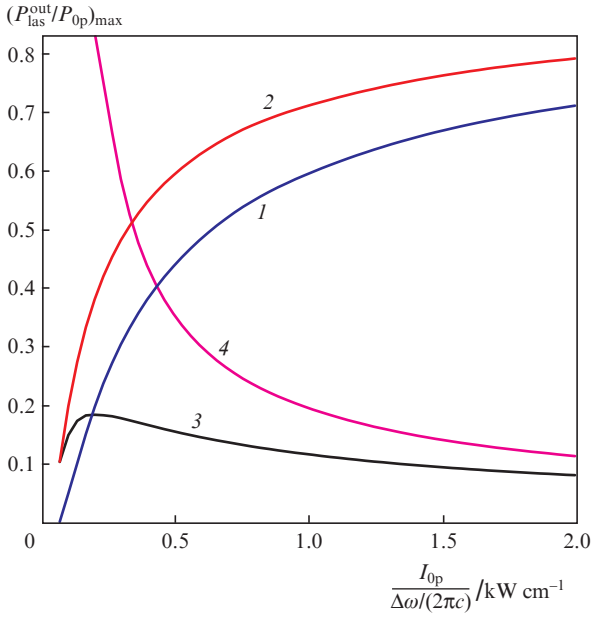

Figure 2. Dependence of the maximum conversion efficiency of pump radiation into laser radiation $(P_{las}^{out}/P_{0p})_{max}$ on the average spectral intensity of pump radiation $I_{0p}/[\Delta\omega/(2\pi c)]$ at optimal parameters $(Ny_0)_{opt}$ and optimum helium pressures p_{He}^{opt}: (*1*) single-sided pumping, (*2*) double-sided pumping with equal height and width of the cell (with $x_0 = y_0$), as well as (*3*) absolute and (*4*) relative increases in laser generation efficiency in passing going from single-sided to double-sided pumping. Calculation parameters are as follows: $T = 395$ K, $p_{CH_4} = 1$ atm, $R_p = 0.99$, $R_0 = 0.3$, $R_1 = 0.99$, $T_0 = 0.99$, $T = 0.99$, $T_s = 0.99$, $\omega_p = \omega_{31}$, $\omega_{las} = \omega_{21}$.

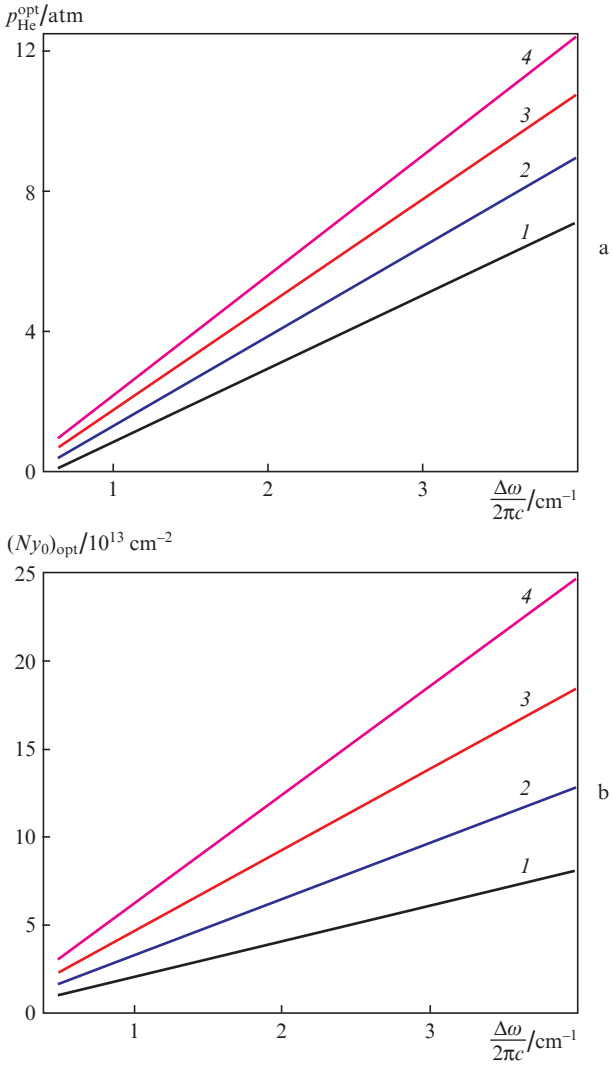

Figure 3. (a) Dependence of the optimal helium pressure p_{He}^{opt} on the half width of the pump emission spectrum $\Delta\omega/(2\pi c)$ at optimal parameters $(Ny_0)_{opt}$ and (b) dependence of the optimal parameter $(Ny_0)_{opt}$ on the half width of the pump emission spectrum at optimum helium pressures p_{He}^{opt}. The values of the average spectral intensity of the pump radiation $I_{0p}/[\Delta\omega/(2\pi c)]$ are (*1*) 0.5 kW cm^{-1} under single-sided pumping; (*2*) 1 kW cm^{-1} under single-sided pumping and 0.5 kW cm^{-1} under double-sided pumping; (*3*) 2 kW cm^{-1} under single-sided pumping and 1 kW cm^{-1} under double-sided pumping; and (*4*) 2 kW cm^{-1} under double-sided pumping. The calculation parameters are the same as in Fig. 2.

Let us discuss condition (27) ($\varkappa_{las} \gg 1 + \varkappa_p + b\varkappa_p\varkappa_{las}$) of the applicability of formulas (42), (43) with the parameters corresponding to Figs 2 and 3. This condition of applicability obviously reduces to two conditions: $\varkappa_{las} \gg 1 + \varkappa_p$ and $b\varkappa_p \ll 1$. In fact, the condition $\varkappa_{las} \gg 1 + \varkappa_p$ is well satisfied in a generator with a large gain length (if the cell is long enough, i.e., if $z_0 \gg x_0, y_0$). The condition $b\varkappa_p \ll 1$ can be met only at a small parameter $b \ll 1$, for which it is necessary to ensure a high

rate of collisional mixing between levels 3 and 2 ($v_{32} \gg \tilde{A}_{21}, \tilde{A}_{31}$). This is achieved by adding methane to the buffer mixture. In our calculations, when the methane pressure is $p_{CH_4} = 1$ atm and in the absence of helium in the buffer mixture, we have $b = 3.68\times10^{-3}$. When helium is added to the buffer mixture, the coefficient b decreases slightly: at $p_{CH_4} = 1$ atm and $p_{He} = 10$ atm, $b = 3.52\times10^{-3}$.

The saturation parameter $\varkappa_p(x,y)$ for the pump radiation depends on the x, y coordinates in the cross section of the cell. It is maximal near the pump diodes, $(\varkappa_p)_{max} = \varkappa_p(0,0)$, and minimal far from the pump diodes, $(\varkappa_p)_{min} = \varkappa_p(x_0,y_0)$. Numerical analysis shows that for a given average spectral intensity of pump radiation, $I_{0p}/[\Delta\omega/(2\pi c)]$ and selected optimal values of $(Ny_0)_{opt}$, p_{He}^{opt} and $p_{CH_4}^{opt}$ at different $\Delta\omega$, the value of the saturation parameter $\varkappa_p$ is the same. For three values of the average spectral pump radiation intensity of 0.5, 1 and 2 kW cm^{-1}, the values of the $b\varkappa_p$ parameter are as follows: $b\varkappa_p(0,0) = 0.09$ and $b\varkappa_p(x_0,y_0) = 0.042$, $b\varkappa_p(0,0) = 0.15$ and $b\varkappa_p(x_0,y_0) = 0.053$, $b\varkappa_p(0,0) = 0.28$ and $b\varkappa_p(x_0,y_0) = 0.068$, respectively. Thus, the condition $b\varkappa_p \ll 1$ in our calculations is fulfilled at an average spectral intensity of pump radiation of no more than 2 kW cm^{-1}.

One can see from Fig. 2 that the generation efficiency of an alkali metal vapour laser increases significantly under double-sided pumping in comparison with single-sided pumping [cf. curves (*1*) and (*2*)]. A maximum increase in efficiency reaches 18% at an average spectral pump radiation intensity of 0.2 kW cm^{-1} [curve (*3*)]. The increase in the generation efficiency slowly decreases with increasing spectral pump radiation intensity: at $I_{0p}/[\Delta\omega/(2\pi c)] = 2$ kW cm^{-1}, an increase in efficiency is 8%. The relative increase in efficiency is higher, the smaller the average spectral intensity of pump radiation: at $I_{0p}/[\Delta\omega/(2\pi c)] = 0.25$ kW cm^{-1}, the relative increase in efficiency reaches 70% [curve (*4*)].

6. Conclusions

We have investigated theoretically the operation of alkali metal vapour lasers under single-sided and double-sided transverse diode pumping. For a practically important case of a sufficiently high intensity of laser radiation, we have obtained analytical formulas that describe the operation of a high-intensity single- and double-sided diode-pumped laser and allow any laser energy characteristics to be exhaustively determined. Comparison of the energy characteristics of single- and double-sided diode-pumped lasers shows that double-sided pumping allows one to increase the conversion efficiency of pump radiation into laser radiation by 8%–18%, and thereby to increase the output power of laser radiation. The physical reason for the increase in laser generation efficiency in passing from single-sided to double-sided pumping is explained by the fact that under conditions (27) of a high intensity of laser radiation, the pump power loss P_{loss} due to spontaneous emission and collisional quenching in the cell volume does not increase with pump power. This leads to an increase in the generation efficiency.

Acknowledgements. The work was carried out at the expense of subsidies for financial support for the fulfilment of the State Task (Project No. AAAA-A17-117052210003-4) at the Institute of Automation and Electrometry, Siberian Branch of the Russian Academy of Sciences and was supported by the RF President's Grants Council (State Support to Leading Scientific Schools Programme, Grant No. NSh-6898.2016.2).

References

1. Krupke F.W. *Progr. Quantum Electron.*, **36**, 4 (2012).
2. Shalagin A.M. *Phys. Usp.*, **54**, 975 (2011) [*Usp. Fiz. Nauk*, **181**, 1011 (2011)].
3. Zhdanov B.V., Knize R.J. *Proc. SPIE*, **8898**, 88980V (2013).
4. Bogachev A.V., Garanin S.G., Dudov A.M., Yeroshenko V.A., Kulikov S.M., Mikaelyan G.T., Panarin V.A., Pautov V.O., Rus A.V., Sukharev S.A. *Quantum Electron.*, **42**, 95 (2012) [*Kvantovaya Elektron.*, **42**, 95 (2012)].
5. Gao F., Chen F., Xie J.J., Li D.J., Zhang L.M., Yang G.L., Guo J., Guo L.H. *Optik*, **124**, 4353 (2013).
6. Pitz G.A., Anderson M.D. *Appl. Phys. Rev.*, **4**, 041101 (2017).
7. Pitz G.A., Stalnaker D.M., Guild E.M., Oliker B.Q., Moran P.J., Townsend S.W., Hostutler D.A. *Proc. SPIE*, **9729**, 972902 (2016).
8. Krupke W.F., Zweiback J.S., Betin A.A. US Patent No. 0022201 Al (2009).
9. Zhdanov B.V., Shaffer M.K., Sell J., Knize R.J. *Opt. Commun.*, **281**, 5862 (2008).
10. Komashko A.M., Zweiback J. *Proc. SPIE*, **7581**, 75810H (2010).
11. Yang Z., Wang H., Lu Q., Li Y., Hua W., Xu X., Chen J. *J. Opt. Soc. Am. B*, **28**, 1353 (2011).
12. Parkhomenko A.I., Shalagin A.M. *Quantum Electron.*, **45**, 797 (2015) [*Kvantovaya Elektron.*, **45**, 797 (2015)].
13. Parkhomenko A.I., Shalagin A.M. *Quantum Electron.*, **47**, 683 (2017) [*Kvantovaya Elektron.*, **47**, 683 (2017)].
14. https://www.nist.gov/pml/atomic-spectra-database.
15. Rotondaro M.D., Perram G.P. *J. Quant. Spectrosc. Radiat. Transfer*, **57**, 497 (1997).
16. Krause L. *Appl. Opt.*, **5**, 1375 (1966).
17. Hrycyshyn E.S., Krause L. *Can. J. Phys.*, **48**, 2761 (1970).
18. Zameroski N.D., Rudolph W., Hager G.D., Hostutler D.A. *J. Phys. B*, **42**, 245401 (2009).
19. Sell J.F., Gearba M.A., Patterson B.M., Byrne D., Jemo G., Lilly T.C., Meeter R., Knize R.J. *J. Phys. B*, **45**, 055202 (2012).